

## Quantitative evaluation of eco-geotechnical measures for debris flow mitigation by improved vegetation-erosion model

LYU Li-qun <sup>1\*</sup>  <https://orcid.org/0000-0002-4430-3594>;  e-mail: Lvliqunqinghua@126.com

XU Meng-zhen <sup>2</sup>  <https://orcid.org/0000-0002-2507-1935>; e-mail: mzxu@mail.tsinghua.edu.cn

ZHOU Guan-yu <sup>1</sup>  <https://orcid.org/0000-0001-9065-9738>; e-mail: Guanyuzhou@bjfu.edu.cn

WANG Zhao-yin <sup>2</sup>  <https://orcid.org/0000-0001-9825-7119>; e-mail: zywang@mail.tsinghua.edu.cn

\*Corresponding author

<sup>1</sup> School of Soil and Water Conservation, Beijing Forestry University, Beijing 100083, China

<sup>2</sup> State Key Laboratory of Hydrosience and Engineering, Tsinghua University, Beijing 100084, China

**Citation:** Lyu LQ, Xu MZ, Zhou GY, et al. (2022) Quantitative evaluation of eco-geotechnical measures for debris flow mitigation by improved vegetation-erosion model. Journal of Mountain Science 19(7). <https://doi.org/10.1007/s11629-021-7285-2>

© Science Press, Institute of Mountain Hazards and Environment, CAS and Springer-Verlag GmbH Germany, part of Springer Nature 2022

**Abstract:** Eco-geotechnical measures for debris flow mitigation and control have attracted wide attention, but the mitigation effect is lack of quantitative evaluation of coordinated measures. In order to evaluate the debris flow mitigation effect in the combinations of geotechnical engineering and ecological engineering, this study investigated the different trends of debris flows behaviour based on the sediment deposition on the gully bed and the loose material on the hillslope. Besides, this research proposed a new model involving vegetation coverage, source gravity energy and debris flow volume based on vegetation-erosion model. The new model validated that the debris flow volume was proportional to the gravity energy of gravel and rock fragments on the hillslope and inversely proportional to the vegetation coverage in a dry-hot valley setting. Furthermore, a typical area in the valley of the Xiaojiang River in Yunnan Province, China was quantified with the new model. The results showed that under different gravity energy conditions, the implementation order of check dam construction and afforestation was important for debris flow mitigation.

**Received:** 21-Dec-2021

**Revised:** 23-Feb-2022

**Accepted:** 29-Apr-2022

**Keywords:** Debris flow; Vegetation coverage; Source energy; Incision and deposition; Afforestation; Check dam; Jiangjia Gully

### 1 Introduction

Debris flows are mixtures of soil, sand, stones, and water that transport large amounts of sediment downstream, which can cause serious damage and economic losses (Lyu et al. 2020). Debris flows often start from landslides and channel bed failures (Gabet and Mudd 2006; Gregoretti and Dalla Fontana 2008; Simoni et al. 2020), moraine lake outbursts (McCoy et al. 2012), and glacial melting (Lyu 2017b).

In some places, hydraulics and geotechnical measures have been adopted to mitigate debris flows, such as check dams, drainage canals, and retaining walls (Ali et al. 2017). Check dams, which are the main hydraulic measure, are constructed across debris flow gullies (Banihabib and Forghani 2017). They are beneficial for reducing flow velocity and soil erosion, controlling sediments and stabilizing gullies (Mekonnen et al. 2015). Check dams could control the

gully incision, thus the potential energy for hillslope erosion was greatly reduced (Wang and Zhang 2019; Wang et al. 2021). Even check dams that are filled by debris flows deposits are useful in mitigating debris flows by reducing the gully bed gradient (Ali et al. 2017).

Afforestation can increase the roughness of debris flows, reduce soil erosion, and facilitate sedimentation. Shen et al. (2016) studied the effect of vegetation restoration on reducing soil erosion and debris flow. Sediments from vegetated land had a higher resistance to be debris flow even under strong rainfall conditions. A combination of trees, shrubs and grass can effectively reduce the solid matter formed by debris flows and increase water infiltration (Cui et al. 2013). The soil apparent shear strength increased in vegetated areas owing to developed root tensile forces and soil-root bonds (Bischetti et al. 2009). Morgan (2009) also showed that vegetation increased the permeability of soil, hence boosting water infiltration and decreasing surface runoff and erosion. In many cases, reinforcement in the root zone is a more important slope stabilizing agent than the effects of transpiration or the creation of preferential flow paths (Sidle and Ochiai 2006). It takes three to five years or more for afforestation to play a significant role in the areas with great potential energy of landslides and creeping (Cui and Lin 2013). However, root systems can also facilitate preferential flow in soils; this can enhance rain age and, thus, dissipate pore water pressure in unstable slope sections (Uchida et al. 2001).

Combination of afforestation and check dams could form a soil and water conservation system, and greatly mitigate debris flow or landslide formation and motion (Promper et al. 2014). Check dams and vegetation development affected erosion and potential energy of the loose material on the hillslope (Lyu 2019; Liang 2020). Wang et al. (2005) developed the vegetation-erosion model, which analyzed the relations among the rate of soil erosion ( $D$ ), vegetation cover ( $V$ ), and human activities. The varying rate of vegetation in Wang's model was proportional to the vegetation but negatively proportional to the erosion rate. However, Wang's model did not consider the potential energy for hillslope erosion. It is necessary to develop a new model including the source energy ( $E$ ) in serious hillslope erosion or gravity erosion area to evaluate

the combined effect of afforestation and check dams for debris flow mitigation. This research used the three tributaries of Jiangjia Gully as a case study to build a model including the source energy to investigate the combined effect of check dams and afforestation on debris flow mitigation. All in all, understanding the effect of eco-geotechnical on hazards mitigation can reduce the capital input and achieve sustained security and stability as well as provide the theoretical guidelines for the design of eco-geotechnical measures.

## 2 Study Area

Jiangjia Gully is a tributary of the Xiaojiang River which, in turn, is a tributary of the Yangtze River, in Yunnan Province, China (Fig. 1). The Xiaojiang Valley is a dry-hot valley with a difference in elevation of more than 3000 m. A dry-hot valley has the characteristics of extremely hot and dry climate due to its specific local climate (Lyu 2019). The vegetation cover in Xiaojiang Valley is severely reduced because of copper mining and logging, which increases debris flows frequency and ecosystem degradation (Lyu 2019; Liang 2020).

The debris flows in Jiangjia Gully occur at high frequencies (up to 28 yr<sup>-1</sup>) and include large flow discharges (maximum 2420 m<sup>3</sup>s<sup>-1</sup>) (Wei et al. 2017). Debris flows blocked the Xiaojiang River seven times between 1957 and 2000, forming a 20-km long barrier lake and destroying fertile fields, railways, highways, and factory facilities along the banks of the river (Wei et al. 2017).

Jiangjia Gully has four tributaries: the Menqian, Duo Zhao, Daozi and Chajing (Fig. 1). The Menqian is the main tributary and the term "upper Jiangjia Gully" refers to this tributary (Fig. 1). In 1974, a check dam was built on the Menqian, but it was destroyed by a debris flow that year. This directly led to an increase in debris flows after 1974. In 1967, 117 check dams were built on the Duo Zhao, but they were destroyed by debris flows in 1974. From 1979 to 1982, another 44 check dams were built on the Duo Zhao, but six of them had been destroyed by 1984 (Fig. 1). The Daozi on the left bank of Jiangjia Gully does not have check dams (Fig. 1). The Chajing tributary was not analyzed because of insufficient data.

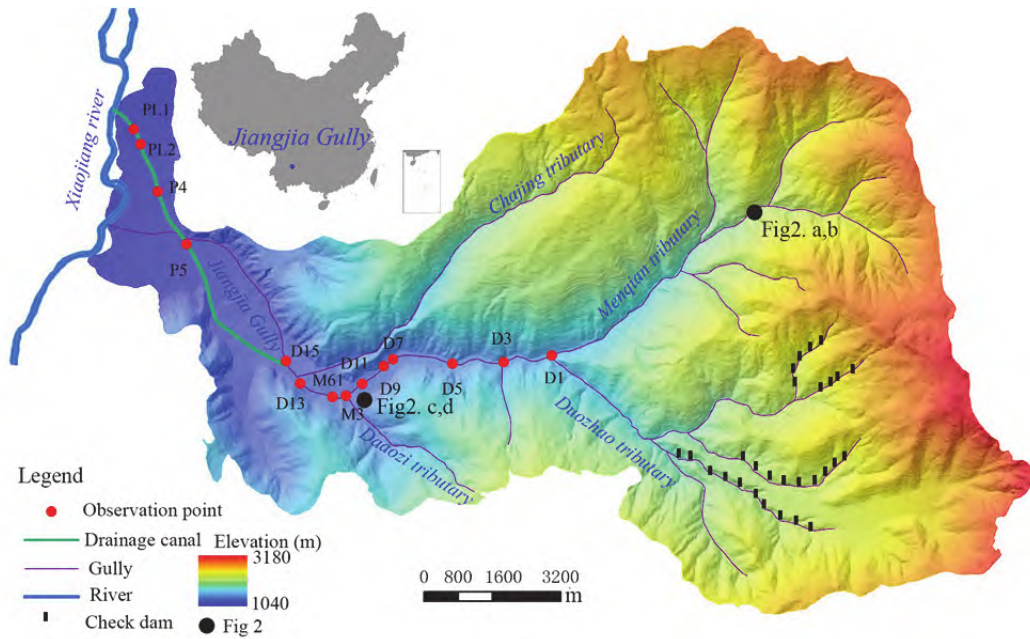


**Fig. 1** Xiaojiang River and Jiangjia Gully, Yunnan Province, China.



**Fig. 2** Jiangjia Gully showing the upstream incision (a, b) and downstream vegetation restoration (c, d) in 2007 and 2020, respectively.

Since the first debris flows in the Jiangjia Gully in 1957, deposition has occurred in the downstream reach of the gully, incision has occurred upstream, and the gully head has retreated (Fig. 2a, b). Since 1980, afforestation has greatly increased the vegetation coverage of Jiangjia Gully (Fig. 2c, d).

Jiangjia Gully can be divided into four parts (Fig.

1): (1) the Menqian and Duo Zhao tributaries (upstream of  $D_1$ ); (2) the part between  $D_1$  and  $D_{11}$  where the width is between 200–300 m; (3) the manual drainage channel ( $P_5$ – $PL_4$ ) where the width is less than 100 m; and (4) the part between  $M_3$  and  $D_{15}$ , where the width is between 300–400 m.

### 3 Methods

Based on the vegetation-erosion model (Wang et al. 2005), the potential energy was added (Fig. 3). The annual volume of debris flows replaced erosion rate in the model, because debris flow (gravity erosion) was the main erosion type in Jiangjia Gully. Debris flow has an eruption cycle, and its volume decreases within a certain period of time after the eruption. Therefore, the change rate of debris flow volume was negative in relation to the volume of the last debris flow (Lyu 2019). The annual volume of debris flows ( $D$ ) was calculated by the thickness of sediments deposition on the gully bed and loose sediments on the hillslope. The vegetation cover ( $V$ ) was obtained by the data from Forestry Bureau and Landsat and MODIS (Fig. 3).

#### 3.1 Thickness of sediments deposition

The bed elevation of the lower Jiangjia Gully between 1964 and 2020 was assessed between the observation points ( $D_1-PL_i$ ) shown in Fig. 1. A geophysical exploration was performed with georadar along Jiangjia Gully ( $D_1-PL_i$ ). This exploration provided the accurate depth of the interface between sediment deposits and the underlying bedrock and gave the thickness of the sediment deposits (Lyu et al. 2020). Although the earliest record of a large debris flow was in 1957, there was no observational data of the bed. The bed elevation of the lower Jiangjia Gully ( $D_1-PL_i$ ) in 1957 was assumed to be the interface between sediment deposits and the underlying bedrock.

The bed elevation upstream of  $D_1$  in the Menqian tributary (in 1957, 1964, 1997, 2005 and 2020), Duozhao tributary (in 1957, 1974, 1982, 1985, 1990 and 2020) and Daaози tributary (in 1957, 1974, 1982, 1985, 2010, and 2020) was taken from Lyu (2019) and Liang (2020).

#### 3.2 Estimating the annual volume of debris flows

Based on the laboratory work of Lyu et al. (2016; 2017a), the volume of the potentially unstable rock mass on the hillslopes was expected to play an important role in the volume of debris flows. Most of sediment transported to the outlet of the gully was originated from the potentially unstable rock mass on the hillslopes (Lyu 2019; Liang 2020). The volume of

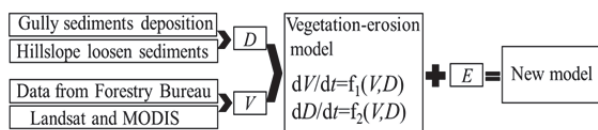


**Fig. 3** Assessment framework about the new vegetation-erosion model based on vegetation cover, debris flows volume and potential energy.

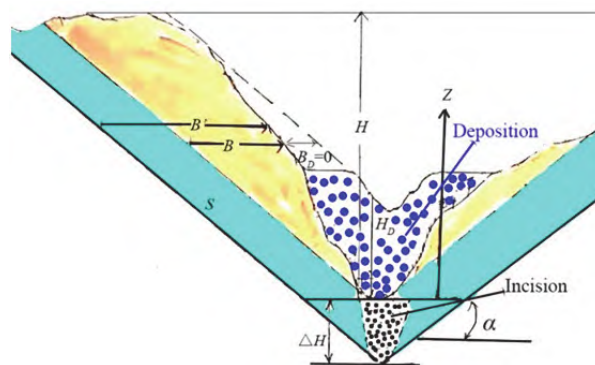


**Fig. 4** Source energy calculation method and the debris flow volume estimation. The circle dot is the siltation behind check dams (blue) and sediment on the gully bed incised (black).  $S$  is the increased area by gully incision.

potentially unstable rock mass on the hillslopes was estimated according to the method introduced by Blothe et al. (2015) in Fig. 4. First, the quantity of potentially unstable rock mass, defined as the rock located between the toe of the hillslope and an idealized topography with slope equal to the threshold hillslope angle,  $\alpha$ , is computed (Fig. 4). Second, the potential volume of debris flow is defined as the increased volume of the potentially unstable rock mass,  $S$ , by gully bed incision (Fig. 4). Third, the proportion of particle percentage in the debris flow and in the original rock mass and soil was used as a measure of soil particle erodibility (Ali et al. 2017). According to the grain size distribution, 10% of the potential volume,  $S$ , flushed into the debris flow per year (Lyu 2019), is estimated as the actual annual debris flow volume,  $D$ . The collapse deposits on the hillslope were loose with average slope angles of 35 (Liu 2010). So, in the present analysis,  $\alpha = 35^\circ$  in this gully was adopted for the potentially unstable rock mass. The slopes on both sides of the tributaries are between  $35^\circ$  and  $65^\circ$ . The debris flow volume of the Menqian (1957, 1964, 1997, 2005 and 2020) and the Duozhao (1957, 1974, 1982, 1985 and 1990) was derived from the changes in the gully bed and potentially unstable rock mass (Fig. 4).

The annual debris flow volume,  $D$  of the Daaози

(1957, 1974, 1982, 1985, 2010 and 2020) was calculated from the elevation change on the Daozi deposition fan (observation point  $M_3$ ).

The total annual debris flow volume,  $D$ , of the main Jiangjia Gully from 1964 to 1999 was taken from Wei et al. (2017).  $D$  of the main Jiangjia Gully from 2000 to 2020 was the product of deposition thickness and deposition area ( $D_1-PL_1$ ).  $D$  of the main Jiangjia Gully in 1957 was estimated as the sediment volume between the underlying bedrock and the bed in 1967.

There are no data about the annual debris flow volume trapped by check dams,  $D_\tau$ , in the Duozhao. However,  $6 \times 10^5 \text{ m}^3$  of sediments were trapped in total from 1974 to 2005. Because the debris flows only occurred in 1974, 1982, 1985, 1990, 1997 and 2005, we assumed that the trapped sediments decreased at a rate of 90% of the dam capacity in each debris flow year (Table 1).

### 3.3 Energy of source material on the hillslope

The debris flow mainly come from the slide of the unstable lateral mass and the mass laying on the channel bed. The kinetic energy of debris flows is related to the transformation of gravitational energy and is released by creeping or by landslides on the hillslope (Weinmeister 2007). If the gully bed is incised down, the value,  $Z$ , will increase. The source energy,  $E$ , will increase (Fig. 4). If the gully bed aggrades due to siltation behind check dams, the source energy,  $E$ , will decrease (Fig. 4). The source energy,  $E$ , above the critical slope,  $\alpha$ , on both hillslopes is calculated as follows (Wang et al. 2021):

$$E = \int_0^H \gamma_s B(z) z dz \quad (1)$$

$$E_{incision} = \int_0^H \gamma_s B'(z) (z + \Delta H) dz \quad (2)$$

$$E_{deposition} = \int_0^H \gamma_s B_D(z) (z - H_D) dz \quad (3)$$

where  $\gamma_s$  is the unit weight,  $B$  is the width,  $B'$  is the width after incision,  $B_D$  is the width after siltation,  $Z$  is the height, and  $H$  is the height of the highest point. For gully incision, the source energy adopts Eq. (2), and  $\Delta H$  is the incision height. For gully deposition, the source energy adopts Eq.(3), and  $H_D$  is the deposition thickness (Fig. 4).

The check dams in the Duozhao tributary were full of sediment until 2005, so the source energy of the Duozhao that was affected by check dams,  $E_\tau$ , can be calculated by the bed elevation change and Eq. (3).

### 3.4 Vegetation coverage

The normalized difference vegetation index (NDVI) is used to represent the vegetation coverage and is recognized as an integrated indicator of elevation change and flood frequency (Casco et al. 2005; Marchetti and Aceñolaza 2012). Positive NDVI values indicate increasing vegetation and negative or zero values indicate water or a surface that has no vegetation. NDVI is a vegetation greenness index sensitive to above-ground biomass. In debris flow gullies, an increase in NDVI reflects the conversion of fresh hillslope surface to vegetation, and enlargement of source material on the hillslope and frequency flood in the gully can be inferred from negative changes in NDVI.

According to the Dongchuan Forestry Bureau, the vegetation coverage of the three tributaries decreased in the 1950s and 1960s due to deforestation. The vegetation coverage rate data,  $V$ , before 1992 came from the Dongchuan Forestry Bureau, and the vegetation coverage rate after 1992 was calculated using NDVI based on Landsat and MODIS (Yang 2018). MODIS is a sensor onboard the Terra and Aqua satellites, with a revisit interval of one or two days. MODIS MOD13Q1 is a 16-day composite remote sensing product, generated by selecting the best data from 16 days. The vegetation recovery was carried out using NDVI time series image datasets with 30 m spatial resolutions. The change in the vegetation coverage rate,  $V_\tau$ , by humans (afforestation and deforestation) from 1957 to 2020 was sourced from the Dongchuan Forestry Bureau (Table 1).

## 4 Results

### 4.1 Debris flow deposition and incision in Jiangjia Gully

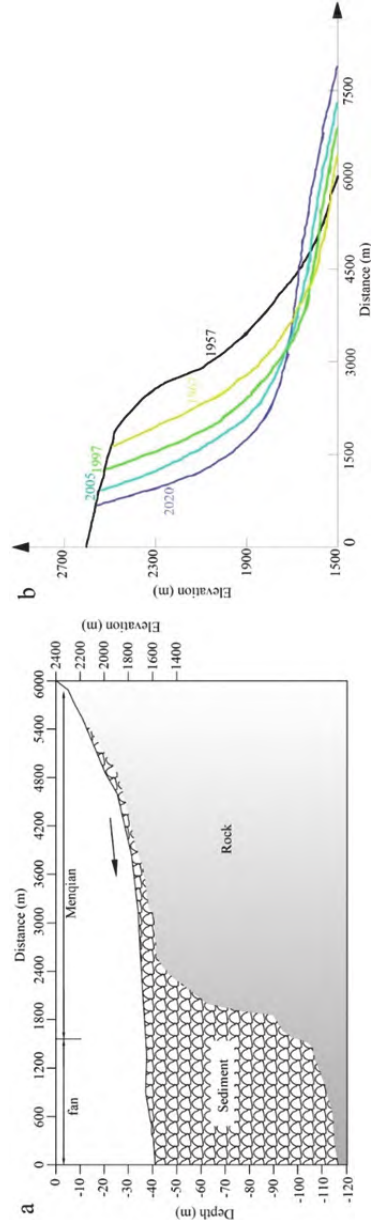
The middle and upper reaches of Jiangjia Gully (upstream of  $D_1$ ) were increasingly incised by debris flows from 1957 to 2005, but the incision rate slowed between 2005 and 2020 (Fig. 5b). The lower reach (downstream of  $D_1$ ) was deposited by the debris flows, which extended into the Xiaojiang River from 1997. The maximum thickness of the debris flow deposition in the lower Jiangjia Gully was 80 m according to the georadar method (Fig. 5a).

Fig. 6 shows the deposition thickness in the lower Jiangjia Gully ( $D_1-PL_1$ ) from 1999 to 2014. The sedimentation thickness reached 23 m and 15 m at  $D_1$

**Table 1** Vegetation coverage, source energy and debris flow volume in the three tributaries

| Parameter                                | Tributary | Year     |          |          |           |           |           |           |           |           |          |          |  |
|--|-----------|----------|----------|----------|-----------|-----------|-----------|-----------|-----------|-----------|----------|----------|--|
|  |           | 1957     | 1964     | 1965     | 1974      | 1982      | 1985      | 1990      | 1997      | 2005      | 2010     | 2020     |  |
| $V$ (-)                                  | Menqian   | 0.2      | 0.18     |          |           |           |           |           | 0.13      | 0.21      | 0.25     | 0.3109   |  |
|  | Duozhao   | 0.2      | 0.12     |          | 0.15      | 0.133     | 0.133     | 0.15      |           | 0.25      | 0.30     | 0.33     |  |
|  | Daozi     | 0.2      |          | 0.12     | 0.02      | 0.11      | 0.132     |           |           | 0.32      | 0.40     | 0.60     |  |
| $V_r$ (-)                                | Menqian   | -0.05    | -0.07    |          |           |           |           |           | 0.005     | 0.01      |          | 0.014    |  |
|  | Duozhao   | -0.05    |          | -0.080   | -0.050    | 0.0140    | 0.010     | 0.010     |           |           | 0.010    | 0.010    |  |
|  | Daozi     | -0.040   |          | -0.080   | -0.050    | 0.0140    | 0.010     |           |           |           | 0.010    | 0.010    |  |
| $E$ (J)                                  | Menqian   | 5.56e+07 | 8.66e+07 |          | 3.00e+07  | 6.60e+06  | 4.16e+06  | 1.69e+06  | 1.13e+08  | 1.23e+08  |          | 8.50e+08 |  |
|  | Duozhao   | 1.63e+07 |          | 1.29e+05 | 2.37e+05  | 2.50e+05  | 2.20e+05  |           |           |           | 1.30e+05 | 9.00e+05 |  |
|  | Daozi     | 1.11e+05 |          | 0        | 0         | 0         | 0         | 0         | 0         | 0         | 0        | 1.20e+05 |  |
| $E_r$ (J)                                | Menqian   | 0        | 0        | 0        | -2.85e+07 | -2.85e+06 | -2.85e+05 | -2.85e+04 | -2.85e+03 | -2.85e+02 | 0        | 0        |  |
|  | Duozhao   | 0        | 0        | 0        | 0         | 0         | 0         | 0         | 0         | 0         | 0        | 0        |  |
|  | Daozi     | 0        | 0        | 0        | 0         | 0         | 0         | 0         | 0         | 0         | 0        | 0        |  |
| $D$ (m <sup>3</sup> yr <sup>-1</sup> )   | Menqian   | 1.31e+06 | 2.01e+06 | 0        | 0         | 0         | 0         | 0         | 0         | 0         | 0        | 0        |  |
|  | Duozhao   | 7.10e+05 | 1.52e+06 | 0        | 1.81e+06  | 5.00e+05  | 4.00e+05  | 3.98e+04  | 3.72e+06  | 5.20e+05  | 0        | 8.00e+05 |  |
|  | Daozi     | 1.00e+04 | 1.50e+04 | 0        | 2.00e+04  | 3.00e+04  | 4.00e+04  | 0         | 0         | 0         | 0        | 0        |  |
| $D_r$ (m <sup>3</sup> yr <sup>-1</sup> ) | Menqian   | 0        | 0        | 0        | 0         | 0         | 0         | 0         | 0         | 0         | 0        | 0        |  |
|  | Duozhao   | 0        | 0        | 0        | -5.4e+05  | -5.4e+04  | -5.4e+03  | -5.4e+02  | -5.4e+01  | -5.4e+00  | 0        | 0        |  |
|  | Daozi     | 0        | 0        | 0        | 0         | 0         | 0         | 0         | 0         | 0         | 0        | 0        |  |

**Notes:**  $V$ , vegetation coverage;  $V_r$ , vegetation coverage affected by afforestation and deforestation;  $D$ , the annual volume of debris flows;  $D_r$ , the annual debris flow volume trapped by check dams;  $E$ , the source energy.  $E_r$ , source energy affected by check dams or incision.



**Fig. 5** Bed elevation of Jiangjia Gully (the Menqian tributary is the upper section of Jiangjia Gully). a. Debris flow deposition thickness in the lower section of Jiangjia Gully; b. Bed elevation of Jiangjia Gully from 1957 to 2020. The bed elevation in 1957 is the rock surface from Fig. 5a, rather than the precise bed elevation. The remaining elevations are modified from Lyu (2019) and Liang (2020).

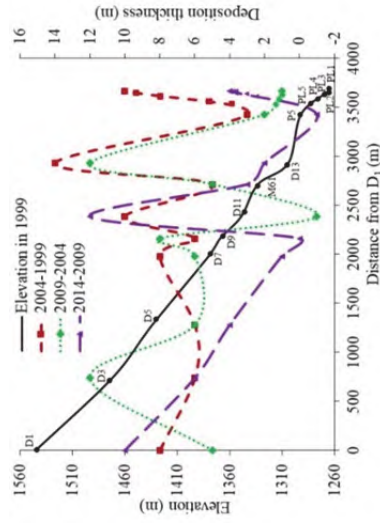


**Fig. 6** Deposition in the lower section of Jiangjia Gully ( $D_1$ - $PL_1$ ) from 1999 to 2014.

and PL<sub>1</sub>. The deposition thickness during 1999–2004, 2004–2009 and 2009–2014 showed retrogressive aggradation by debris flows. The points of PL<sub>1</sub>–M<sub>61</sub> showed more siltation from 1999 to 2004, but D<sub>3</sub>–D<sub>9</sub> showed more siltation from 2004 to 2009.

**4.2 Performance of check dams in trapping debris flows sediment**

The estimated total volume of the debris flow from the outlet of Jiangjia Gully in 1957 was 2.31 million m<sup>3</sup>, although the real volume would have been smaller. Debris flow volumes were small between 1964 and 1974, increased between 1974 and 1990, and decreased between 2000 and 2019 (Fig. 7a).

Debris flow volume in the Duozhao tributary was 0.71 million m<sup>3</sup> in 1957, and decreased from 0.04 million m<sup>3</sup> in 1985 to 0 million m<sup>3</sup> in 2020 (Fig. 7b). The check dams mitigated the debris flow significantly in the Duozhao tributary. Debris flow volumes in the Menqian tributary were between 0.52 and 1.31 million m<sup>3</sup> from 1957 to 2020. Debris flow volumes in the Daozi tributary were between 0.006 and 0.04 million m<sup>3</sup> from 1957 to 2020. The debris flow volume in the Menqian and Daozi tributary changed little due to the lack of check dam’s construction (Fig. 7b).

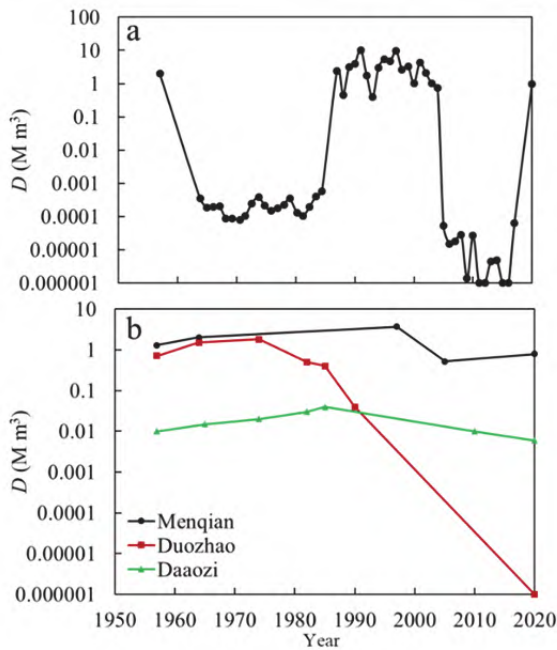


**Fig. 7** Annual volume of debris flow in the main Jiangjia Gully (a) and in the three tributaries (b).

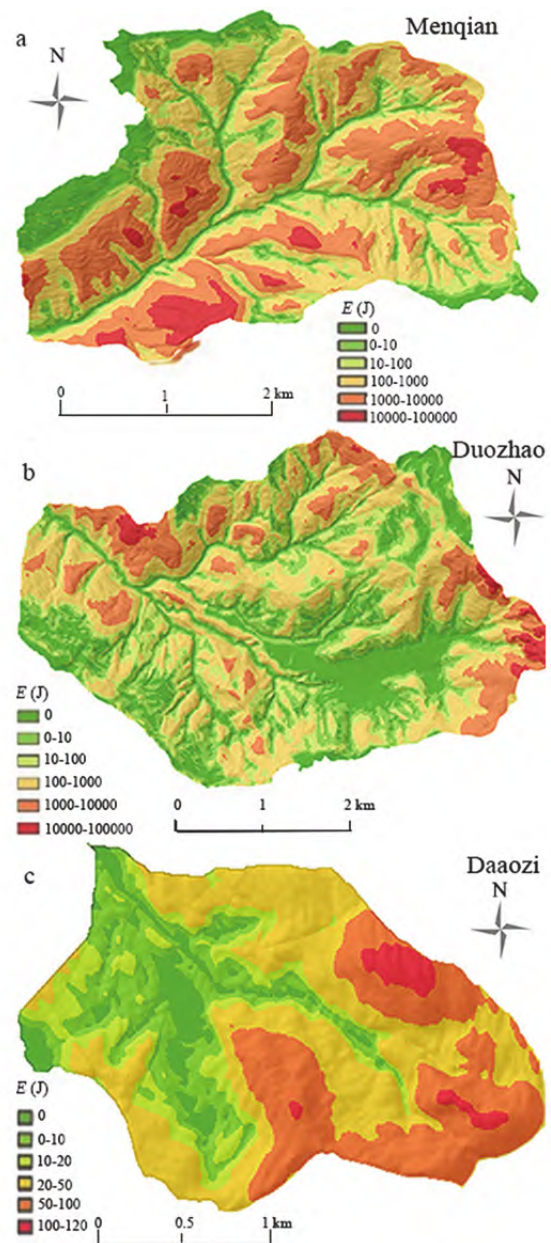


**Fig. 8** Source energy distribution of the three tributaries in 2020.

**4.3 Effect of check dams on the source energy for debris flows**

The source energy of the Menqian tributary was high compared with the Duozhao tributary due to the lack of check dam construction (Fig. 8). Fig. 9 shows the total energy of the Menqian, Duozhao and Daozi tributaries from 1957 to 2020. The source energy of the Duozhao tributary gradually decreased after 1970 because of check dam construction. However, the source energy of Menqian and Daozi changed little.

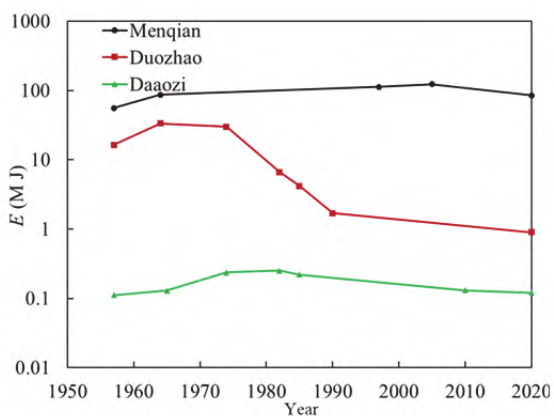


**Fig. 9** Source energy of the three tributaries from 1957 to 2020.

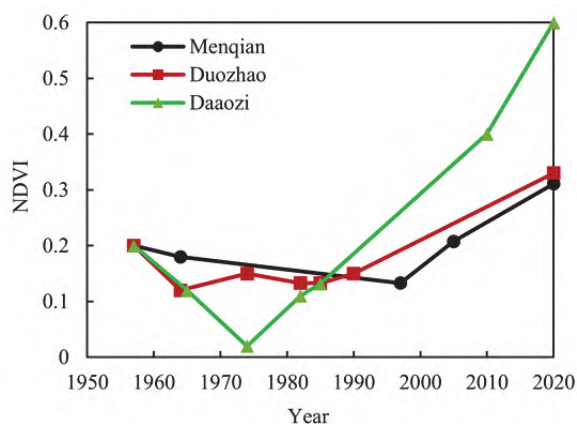


**Fig. 11** Vegetation coverage of the three tributaries with 30 m spatial resolutions from 1957 to 2020.

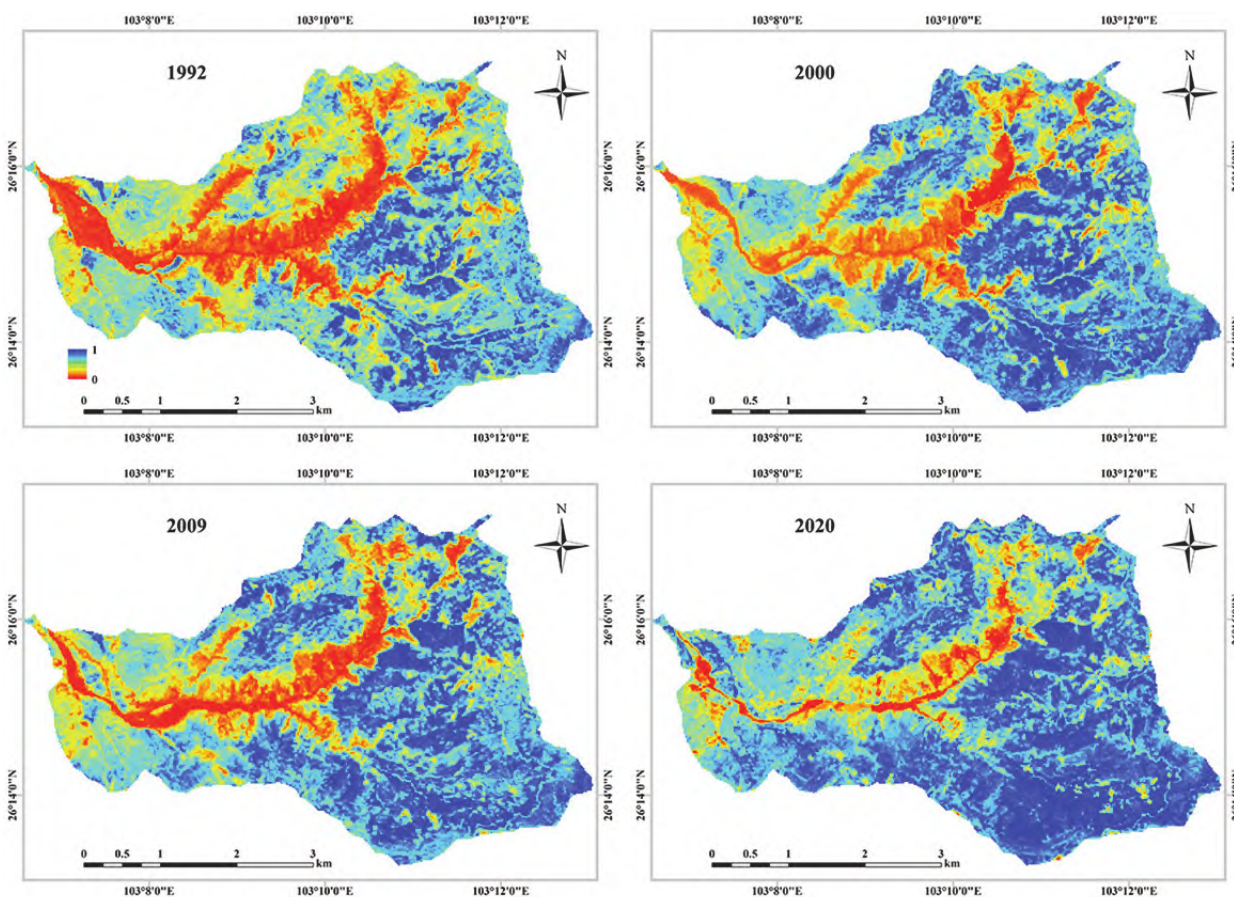


**Fig. 10** Vegetation coverage of Jiangjia Gully in 1992, 2000, 2009 and 2020.

**4.4 Change of vegetation coverage due to check dams and afforestation**

Fig. 10 shows that the vegetation coverage of Jiangjia Gully over the catchments of the tributaries continued to improve. From 2000, the

vegetation coverage was quickly restored through afforestation; in particular, the vegetation coverage of the Daozi has increased significantly. Only the Menqian and the lower reaches of Jiangjia Gully were below 0.4 vegetation coverage. By 2020, with the construction of check dams and afforestation, 80% of

the Duozhao tributary had vegetation coverage above 0.4 (Fig. 10). Fig. 11 shows that the vegetation coverage increase quickly from 2000. Especially in the Daaози tributary, the vegetation coverage was between 0.3 and 0.4, which was higher than the vegetation coverage over the other two tributaries between 0.12 and 0.3.

**4.5 New evaluation model for debris flow mitigation**

The change rate of debris flow volume in Jiangjia Gully,  $D' = dD/dt$ , was negative with the increase of vegetation coverage,  $V$ , and positive with the increase of the source energy,  $E$  (Fig. 7, 9 and 11). The change rate of source energy,  $E' = dE/dt$ , was negative because of the increase of vegetation coverage,  $V$ , and was positive because of the increase of the debris flow volume,  $D$  (Fig. 7, 9 and 11). The change rate of vegetation coverage,  $V' = dV/dt$  was negatively to source energy (Fig. 9 and 11). The varying rates of source energy and debris flow volume were also assumed to be linear with other factors. Eq. (4) was established based on vegetation-erosion model, and the above relations between  $V, E$  and  $D$ .

$$\left. \begin{aligned} \frac{dV}{dt} - aV + cE + gD &= V_{\tau} \\ \frac{dE}{dt} - bE + fV - hD &= E_{\tau} \\ \frac{dD}{dt} + iD + jV - kE &= D_{\tau} \end{aligned} \right\} \quad (4)$$

where parameter  $a$  depends on the local rainfall, environmental and plant composition;  $c$  represents the destructive effect of source energy on vegetation;  $g$  represents the destructive effect of the debris flow volume on vegetation;  $b$  depends on the local source energy;  $f$  represents the effect of vegetation coverage on source energy;  $h$  represents the effect of incision by debris flow on the source energy;  $i$  represents the impact of the debris flow volume on the next debris flow volume;  $j$  represents the inhibitory effect of vegetation on debris flow volume, where the increase in vegetation coverage is beneficial; and  $k$  represents

the promoting effect of the source energy on the debris flow volume.

Using values of vegetation coverage,  $V$ , source energy,  $E$ , debris flow volume  $D$ , and human activities on vegetation coverage,  $V_{\tau}$ , source energy,  $E_{\tau}$ , debris flow volume,  $D_{\tau}$ , in Table 1, and Eq. (4), the values of parameters  $a, b, c, f, g, h, i, j$ , and  $k$  were obtained by the software Opt8.0 which used global optimization algorithm for nonlinear fitting of partial differential equations (Li and Wang 2016).

Table 2 shows that parameters  $a, j$ , and  $f$  were highest in the Daaози tributary, which indicates that vegetation coverage had the greatest impact on the debris flow control in the Daaози. The maximum values of parameters  $b, c$ , and  $k$  were in the Duozhao, which indicates that, here, check dam construction had the greatest impact on debris flow control. Owing to the construction of the check dams in the Duozhao, the destructive effect of debris flow on vegetation coverage was small, and most trees survived, so the value of  $g$  in the Duozhao was the lowest. By substituting the values for parameters, vegetation coverage, and source energy in Table 2 into Eq. (4) to calculate the debris flow volume in different years, Fig. 12 shows that the calculated value and the actual value were consistent for the debris flow trend.

**5 Discussion**

**5.1 Application of the new evaluation model**

The  $V-E$  plane in Fig. 12 can be divided into three zones by the lines  $V' = dV/dt = 0$  and  $E' = dE/dt = 0$ , (Fig. 13), as follows.

- (1) Zone A ( $V' < 0, E' > 0$ ): The vegetation coverage is decreasing and the source energy is increasing. This is the area in which debris flow disasters are aggravated.
- (2) Zone B ( $V' > 0, E' > 0$ ): The vegetation coverage is increasing and the source energy is increasing. This is the transition area for debris flow disasters.
- (3) Zone C ( $V' > 0, E' < 0$ ): The vegetation coverage is increasing and the source energy is decreasing. This

**Table 2** Dynamics model parameters of vegetation coverage–source energy–debris flow volume

| Tributary | Parameter               |                           |                        |                         |                          |                         |                         |  |  |
|-----------|-------------------------|---------------------------|------------------------|-------------------------|--------------------------|-------------------------|-------------------------|--|--|
|           | $a$ (yr <sup>-1</sup> ) | $c$ (J·yr <sup>-1</sup> ) | $g$ (m <sup>-3</sup> ) | $b$ (yr <sup>-1</sup> ) | $f$ (Jyr <sup>-1</sup> ) | $h$ (Jm <sup>-3</sup> ) | $i$ (yr <sup>-1</sup> ) | $j$ (m <sup>3</sup> yr <sup>-2</sup> ) | $k$ (m <sup>3</sup> J <sup>-1</sup> yr <sup>-2</sup> ) |
| Menqian   | 2.96e-01                | 1.17e-18                  | 7.82e-18               | 6.21e-43                | 5.77e+01                 | 1.56e-08                | 2.12e+02                | 1.85e-01                               | 3.83e-03   |
| Duozhao   | 7.48e-01                | 2.75e-09                  | 2.67e-39               | 5.52e-02                | 6.02e+03                 | 8.94e+00                | 1.17e-41                | 1.26e+02                               | 1.17e+00   |
| Daaози    | 1.27e+00                | 2.21e-19                  | 1.75e-17               | 2.43e-02                | 1.81e+04                 | 5.09e-15                | 5.72e-12                | 1.15e+03                               | 6.86e-05   |

is the area in which debris flow disasters are reduced.

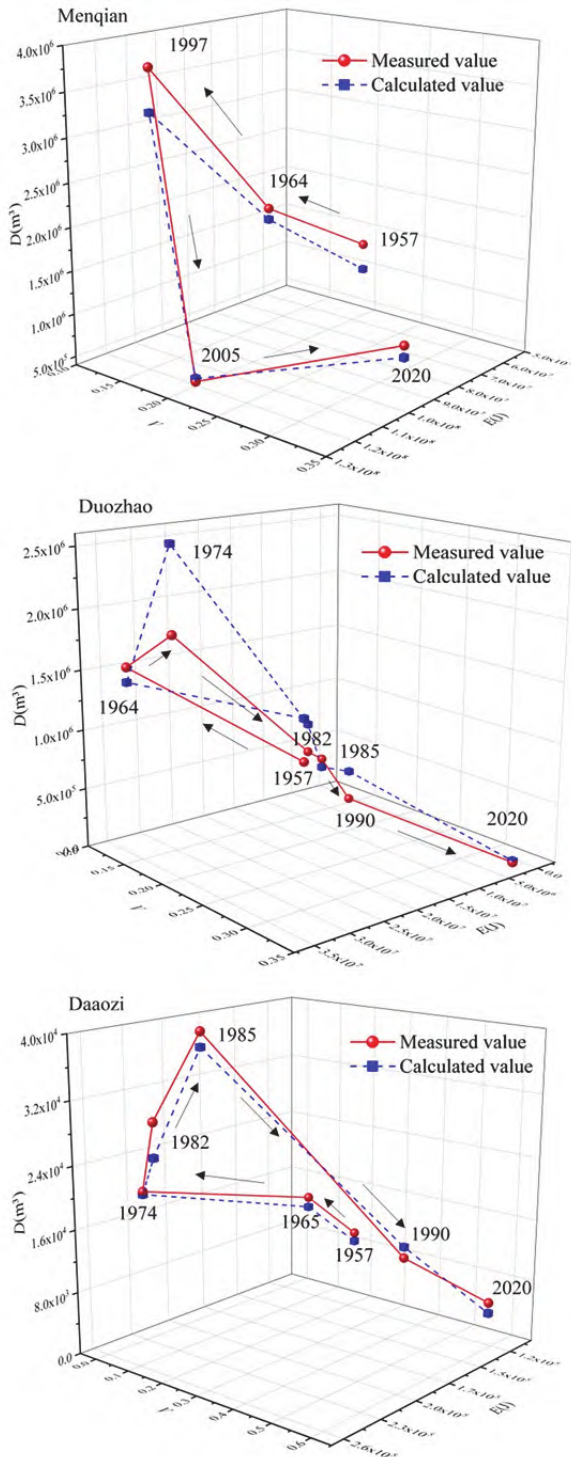


**Fig. 12** Relationship between debris flow volume ( $D$ ), source energy ( $E$ ) and vegetation coverage ( $V$ ) in the three tributaries from 1957 to 2020.

For the Menqian and Duozhao tributaries, which had higher source energy, afforestation cannot fully control debris flow. Check dams should be

constructed first to reduce the source energy. Then afforestation can disrupt the accumulation of material sources, and control debris flows (such as in the Duozhao tributary). For tributaries with a low source energy, afforestation can control debris flows (such as in the Daozi tributary).

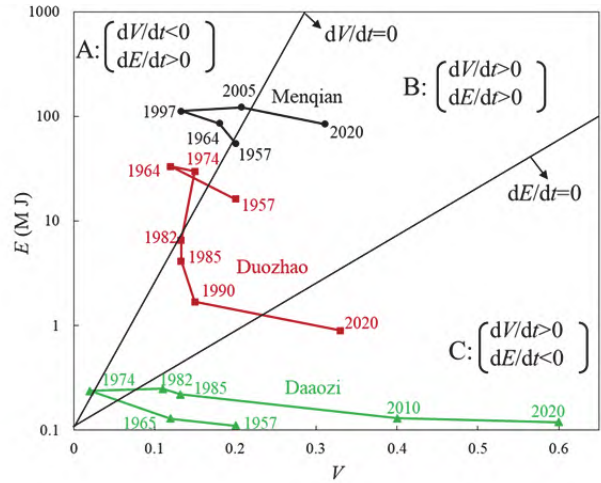


**Fig. 13** Three zones of source energy–vegetation coverage plane in the three tributaries from 1957 to 2020.

The vegetation coverage–source energy–debris flow volume dynamics model in Eq. (4) may be representative for similar debris flow processes in serious hillslope erosion or gravity erosion area and dry-hot valleys. There were spatial differences in the physical and mechanical properties of different combinations of vegetation and rock–soil media in the dry-hot valleys. Therefore, the parameters in the vegetation coverage–source energy–debris flow volume dynamics model differed. Obtaining parameter values in different regions through field surveys and indoor experiments can guide combined models of check dam construction and afforestation in different dry-hot valleys.

### 5.2 Limitations of the new evaluation model

Fig. 7 and 9 showed that the debris flow volume in Duozhao tributary decreased quickly as the energy of source material on the hillslope decreased due to check dam construction. The check dams were full deposition from 1990. The debris flow volume in Duozhao tributary continue to decrease as the energy of source material changed little from 1990. The old check dams with full deposition can still be useful in controlling debris flows, which is consistent with the

conclusion by Ali et al. (2017).

The vegetation growth may be another reason for the inconsistent pace between the debris flow volume decrease and the energy decrease of source material from 1990. As the afforestation and vegetation growth, the soil shear strength is found to increase due to the developed root tensile forces and soil-root bonding (Wu et al. 1979; Bischetti et al. 2009). Morgan (2009) showed that vegetation decreases surface water runoff and sediment erosion. Compared with the bare slope, the vegetated deposits have higher erosion resistance and are resistant to erosion even under more intense rainfall (Shen et al. 2017). Hence, the threshold hillslope angle,  $\alpha$ , in Fig. 4 has increased due to the vegetation growth and decreased the energy of source material. In this study, the changes of threshold hillslope angle due to vegetation are not considered.

In the new model, the change rate of debris flow volume, source energy and vegetation coverage were assumed to be linear with other factors. The geotechnical measures in this study area were only check dams. In serious hillslope erosion or gravity erosion area, check dams, drainage canals, and retaining walls might be adopted comprehensively. So the new model in the future should consider the role of different geotechnical measures on the source energy, vegetation coverage and debris flow volume. And the more accurate relationship between the change rate of debris flow volume, source energy, vegetation coverage should be calculated carefully using demo data by improved vegetation-erosion model.

## 6 Conclusion

The good performance of the new model supports the physical interpretation of the debris flow trends in the Jiangjia Gully. Debris flow volume was proportional to the source energy and inversely proportional to the vegetation coverage. Owing to the different combinations of check dams and

afforestation in the three tributaries, the trend of debris flow development differed. Check dam construction and afforestation worked simultaneously in the Duozhao while afforestation was the main reason for the debris flow reduction in the Daozi. As the main tributary of Jiangjia Gully, the Menqian tributary had only one check dam, which was destroyed in 1974. Afforestation did not seem to control debris flows in this tributary. The vegetation coverage–source energy–debris flow volume dynamics model could explain the effect of different factors on the trends of debris flow development in the three tributaries. Using only afforestation in low source energy gullies can control debris flow, whereas high source energy gullies require the construction of check dams first, followed by afforestation. Check dams function was not just by storing sediment but by promoting vegetation and reducing slopes and available energy. However, the factors in the new model were assumed to be linear with each other and did not consider the other geotechnical engineering measures like drainage canals, and retaining walls. The quantitative assessment of eco-geotechnical measures for debris flow mitigation should base on a comprehensive model considering the accurate relationship of the factors and all kinds of geotechnical measures in the future.

## Acknowledgments

This study is supported by the National Natural Science Foundation of China (41790434 and 41907229), the Second Tibetan Plateau Scientific Expedition and Research Program (STEP) (2019QZKK0903), Chinese Academy of Sciences (XDA23090401), and the National Key R & D Program of China (2018YFC1505201). We also gratefully acknowledge the Beijing Municipal Education Commission for their financial support through Innovative Trans disciplinary Program “Ecological Restoration Engineering”.

## References

- Ali RV, Mohammad A, Saskia K, et al. (2017) Assessment of soil particle erodibility and sediment trapping using check dams in small semi-arid catchments. *Catena* 157: 227–240. <https://doi.org/10.1016/j.catena.2017.05.021>.
- Banihabib ME, Forghani A (2017) An assessment framework for the mitigation effects of check dams on debris flow. *Catena*

- 152: 277–284. <https://doi.org/10.1016/j.catena.2017.01.018>
- Blothe JH, Korup O, Schwanghart W (2015) Large landslides lie low: Excess topography in the Himalaya-Karakoram ranges. *Geology* 43(6):523–526. <https://doi.org/10.1130/G36527.1>

- Bischetti GB, Chiaradia EA, Epis T (2009) Root cohesion of forest species in the Italian Alps. *Plant Soil* 324 (1-2): 71-89. <https://doi.org/10.1007/s11104-009-9941-0>
- Casco SL, Chiozzi NI, Neiff JJ (2005) La vegetación como indicador de la geomorfología fluvial. *Revista Brasileira de Geomorfologia* 6 (1): 123-136. <https://doi.org/10.20502/rbg.v6i1.46>
- Cui P, Li YM (2013) Debris-Flow Treatment: The Integration of Botanical and Geotechnical Methods. *J Resour Ecol* 4 (2): 97-104. <https://doi.org/10.5814/j.issn.1674-764x.2013.02.001>
- Gabet EJ, Mudd SM (2006) The mobilization of debris flows from shallow landslides. *Geomorphology* 74 (1-4): 207-218. <https://doi.org/10.1016/j.geomorph.2005.08.013>
- Gregoretti C, Fontana GD (2008) The triggering of debris flow due to channel-bed failure in some alpine headwater basins of the dolomites: analyses of critical runoff. *Hydrol Process* 22 (13): 2248-2263. <https://doi.org/10.1002/hyp.6821>
- Liang XY, Xu MZ, Lyu LQ, et al. (2020) Geomorphological characteristics of debris flow gullies on the edge of the Qinghai-Tibet Plateau. *Acta Geogr Sin* 75 (75): 1373-1382. (In Chinese) <https://doi.org/10.11821/dlxb202007004>
- Liu DD (2010) Study on the Grain Erosion and Control Strategy in the Southwest Dry Valley. MA thesis, Tsinghua University, Beijing. p 20. (In Chinese)
- Lyu LQ, Wang ZY, Cui P (2016) Mechanism of the intermittent motion of two-phase debris flows. *Environ Fluid Mech* 17 (1): 139-158. <https://doi.org/10.1007/s10652-016-9483-y>
- Lyu LQ, Wang ZY, Cui P, et al. (2017) The role of bankerosion on the initiation and motion of gully debris flows. *Geomorphology* 285, 137-151. <https://doi.org/10.1016/j.geomorph.2017.02.008>
- Lyu LQ (2017) Research on the initiation and motion of gully debris flows in Tibetan Plateau. PhD thesis, Tsinghua University, Beijing. p 20. (In Chinese)
- Lyu LQ (2019) Debris flow activities and their role on geomorphological evolution in deep valleys of Qinghai-Tibet plateau. Postdoctoral Research Report, Tsinghua University, Beijing. pp 76-78. (In Chinese)
- Lyu LQ, Xu MZ, Wang ZY, et al. (2021) Impact of densely distributed debris flow dams on river morphology of the Grand Canyon of the Nu River (upper Salween River) at the east margin of the Tibetan Plateau. *Landslides* 18: 979-991. <https://doi.org/10.1007/s10346-020-01536-x>
- Marchetti ZY, Aceñolaza PG (2012) Pulse regime and vegetation communities in fluvial systems: The case of the Parana River floodplain, Argentina. *Flora-Morphology, Distribution, Functional Ecology of Plants* 207 (11): 795-804. <https://doi.org/10.1016/j.flora.2012.09.004>
- Mekonnen M, Keesstra SD, Stroosnijder L, et al. (2015) Soil conservation through sediment trapping: a review. *Land Degrad Dev* 26 (6): 544-556. <https://doi.org/10.1002/ldr.2308>
- McCoy SW, Kean JW, Coe JA, et al. (2012) Sediment entrainment by debris flows: in situ measurements from the headwaters of a steep catchment. *J Geophys Res: Earth Surf* F3: F03016. <https://doi.org/10.1029/2011JF002278>
- Morgan RPC (2009) *Soil Erosion and Conservation* John Wiley and Sons. New York, USA.
- Promper C, Puissant A, Malet JP (2014) Analysis of land cover changes in the past and the future as contribution to landslide risk scenarios. *Appl Geogr* 53: 11-19. <https://doi.org/10.1016/j.apgeog.2014.05.020>
- Shen P, Zhang LM, Chen HX, et al. (2016) Role of vegetation restoration in mitigating hillslope erosion and debris flows. *Eng Geol* 216: 122-133. <https://doi.org/10.1016/j.enggeo.2016.11.019>
- Sidle RC, Ochiai H (2006) *Landslides: Processes, Prediction, and Land Use*. Water Resources Monograph. American Geophysical Union, Washington. p 312. <https://doi.org/10.1029/WM018>
- Simoni A, Bernard M, Berti M, et al. (2020) Runoff - generated debris flows: observation of initiation conditions and erosion - deposition dynamics along the channel at Cancia (eastern Italian Alps). *Earth Surf Process Landf* 45(14): 3556-3571. <https://doi.org/10.1002/esp.4981>
- Uchida T, Kosugi K, Mizuyama T (2010) Effects of pipeflow on hydrological process and its relation to landslide: a review of pipeflow studies in forested headwater catchments. *Hydrol Process* 15: 2151-2174. <https://doi.org/10.1002/hyp.281>
- Wang ZY, Chen ZY, Yu S, et al. (2021) Erosion-control mechanism of sediment check dams on the Loess Plateau. *Int J Sediment Res* 36(5): 668-677. <https://doi.org/10.1016/j.ijsrc.2021.02.002>
- Wang ZY, Wang GQ, Li CZ (2005) A preliminary study on vegetation-erosion dynamics and its applications. *Sci China - Series D: Earth Sci* 48(5): 689-700. <https://doi.org/10.1360/03yd0074>
- Wang ZY, Zhang CD (2019) Mechanism of energy dissipation and hazard mitigation of riverbed structures in southwestern China. *Chin J Hydraul Eng* (1): 124-134. (In Chinese) <https://doi.org/10.13243/j.cnki.slxb.20181081>
- Wei L, Hu KH, Li XY, et al. (2017) Inter-annual Variation of the Morphology of Debris Flow Channel in Jiangjia Gully. *J Yangtze River Sci Res Inst* 34 (9): 57. (In Chinese)
- Weinmeister H (2007) Integrated debris flow disaster mitigation. *J Mt Sci* 4: 293-308. <https://doi.org/10.1007/s11629-007-0293-z>
- Wu TH, McKinnell III WP, Swanston DN (1979) Strength of tree roots and landslides on Prince of Wales Island, Alaska. *Can Geotech J*. 16 (1): 19-33. <https://doi.org/10.1139/t79-003>
- Yang WT, Qi WW, Zhou JX (2018) Decreased post-seismic landslides linked to vegetation recovery after the 2008 Wenchuan earthquake. *Ecol Indic* 89: 438-444. <https://doi.org/10.1016/j.ecolind.2017.12.006>